BIG Regulates Dynamic Adjustment of Circadian Period in *Arabidopsis thaliana*[1][CC-BY]

Timothy J. Hearn,[a] Maria C. Marti Ruiz,[a] S.M. Abdul-Awal,[a,b] Rinukshi Wimalasekera,[a] Camilla R. Stanton,[a] Michael J. Haydon,[c] Frederica L. Theodoulou,[d] Matthew A. Hannah,[e] and Alex A.R. Webb[a,2,3]

[a]Department of Plant Sciences, University of Cambridge, Cambridge CB2 3EA, United Kingdom
[b]Biotechnology and Genetic Engineering Discipline, Khulna University, Khulna-9208, Bangladesh
[c]School of BioSciences, University of Melbourne, Melbourne, Victoria 3010, Australia
[d]Plant Sciences Department, Rothamsted Research, Harpenden AL5 2JQ, United Kingdom
[e]BASF Agricultural Solutions Belgium NV, 9052 Ghent, Belgium

ORCID IDs: 0000-0001-6827-4196 (T.J.H.); 0000-0003-1698-1168 (M.C.M.R.); 0000-0002-8807-624X (S.A.-A.); 0000-0002-5777-4969 (C.R.S.); 0000-0003-2486-9387 (M.J.H.); 0000-0002-8306-0716 (F.L.T.); 0000-0002-4889-490X (M.A.H.); 0000-0003-0261-4375 (A.A.W.)

Circadian clocks drive rhythms with a period near 24 h, but the molecular basis of the regulation of the period of the circadian clockis poorly understood. We previously demonstrated that metabolites affect the free-running period of the circadian oscillator of Arabidopsis (*Arabidopsis thaliana*), with endogenous sugars acting as an accelerator and exogenous nicotinamide acting as a brake. Changes in circadian oscillator period are thought to adjust the timing of biological activities through the process of entrainment, in which the circadian oscillator becomes synchronized to rhythmic signals such as light and dark cycles as well as changes in internal metabolism. To identify the molecular components associated with the dynamic adjustment of circadian period, we performed a forward genetic screen. We identified Arabidopsis mutants that were either period insensitive to nicotinamide (*sin*) or period oversensitive to nicotinamide (*son*). We mapped *son1* to *BIG*, a gene of unknown molecular function that was shown previously to play a role in light signaling. We found that *son1* has an early entrained phase, suggesting that the dynamic alteration of circadian period contributes to the correct timing of biological events. Our data provide insight into how the dynamic period adjustment of circadian oscillators contributes to establishing a correct phase relationship with the environment and show that BIG is involved in this process.

The circadian clock is an endogenous oscillator that, in Arabidopsis (*Arabidopsis thaliana*), consists of nuclear and cytosolic feedback loops. It is often considered that the circadian oscillator runs with a period of 24 h, but the circadian period is plastic, depending on environmental conditions. For example, in diurnal organisms such as Arabidopsis, the circadian clock has a reduced period with increased light intensity (Aschoff, 1960). This is commonly referred to as Aschoff's rule and was the foundation for the model of parametric entrainment that describes how the circadian oscillator synchronizes with environmental cycles (Aschoff, 1960). We have discovered that exogenous application of two common metabolites also regulates the circadian period in Arabidopsis. Suc reduces the circadian period under dim light conditions (Haydon et al., 2013), whereas nicotinamide makes the circadian clock run more slowly, with a period near 27 h (Dodd et al., 2007).

The way in which circadian clocks regulate and adjust the circadian period is unknown. We refer to this ability of the circadian clock to adapt to environmental conditions as dynamic adjustment of circadian period. To investigate this dynamic adjustment, we have used nicotinamide as a tool that increases the circadian period. Previously, we proposed that nicotinamide affects circadian period through its action as an antagonist of Ca^{2+} signaling (Dodd et al., 2007). There is circadian regulation of cytosolic free calcium ($[Ca^{2+}]_{cyt}$) in mesophyll cells (Martí et al., 2013), and this encodes information about light intensity and quality (Love et al., 2004; Xu et al., 2007). In Arabidopsis, circadian regulation of $[Ca^{2+}]_{cyt}$ is driven by the second messenger cADP ribose (cADPR) under the control of the morning oscillator gene *CIRCADIAN CLOCK ASSOCIATED1* (*CCA1*; Dodd et al., 2007; Xu et al., 2007). Nicotinamide, the by-product of cADPR synthesis, inhibits both cADPR accumulation (Dodd et al., 2007) and ADPR cyclase activity (Abdul-Awal et al., 2016). There is no gene in Arabidopsis with homology to any of the known ADPR cyclases (Hunt et al.,

[1]T.J.H. was supported by Biotechnology and Biological Sciences Research Council (BBSRC) CASE studentship 1090203 supported by Bayer Cropscience and BBSRC Grant BB/M006212/1. M.C.M. was supported by a University of Cambridge Broodbank Fellowship.

[2]Author for contact: aarw2@cam.ac.uk.
[3]Senior author.
The author responsible for distribution of materials integral to the findings presented in this article in accordance with the policy described in the Instructions for Authors (www.plantphysiol.org) is: Alex A.R. Webb (aarw2@cam.ac.uk).

T.J.H., M.J.H., M.A.H., and A.A.R.W. devised the study; T.J.H., S.M.A.-A., C.R.S., R.W., and M.C.M. conducted the experiments; T.J.H., M.C.M., F.L.T., and A.A.R.W. wrote the article.

www.plantphysiol.org/cgi/doi/10.1104/pp.18.00571

2007). However, the existence of a completely novel ADPR cyclase in the green lineage cannot be ruled out, as many cyclases have yet to be characterized at the genetic level in mammals (Masuda et al., 1997).

Nicotinamide increases circadian period in all organisms tested, including Arabidopsis (Dodd et al., 2007), mouse (Asher et al., 2008), and *Ostreococcus tauri* (O'Neill et al., 2011). In animals, nicotinamide has been hypothesized to affect both circadian period and amplitude through the inhibition of poly-ADP-ribose polymerase (Ramsey et al., 2009) or SIRTUINs (Asher et al., 2008). Similar to ADPR cyclase, SIRTUINS are enzymes belonging to the NADase superfamily that release nicotinamide as a by-product of ADPR production. However, consistent with the effect of nicotinamide on circadian period being due to the inhibition of ADPR cyclase, a knockout mutation of *CD38*, the main mammalian ADPR cyclase, causes a long circadian period in mice (Sahar et al., 2011).

We have used nicotinamide as a tool to understand the potential mechanisms that regulate the dynamic adjustment of circadian period and to determine how nicotinamide regulates the circadian clock. We performed a forward genetic screen to identify loci that affect the sensitivity of the circadian oscillator to nicotinamide. Previous genetic analyses of the circadian system have focused on the identification of components of the circadian oscillator through screens for a short or long circadian period in constant light (Millar et al., 1995; Somers et al., 2000; Panda et al., 2002; Hazen et al., 2005) or constant darkness (Kevei et al., 2007; Martin-Tryon et al., 2007; Hong et al., 2010; Ashelford et al., 2011). We have taken a different approach by screening for mutations that are affected in their ability to change circadian period in response to altered conditions. We predicted that such a screen might identify genes involved in the response to nicotinamide and, more importantly, genes that participate in the dynamic adjustment of circadian period. We report the mapping by sequencing of an Arabidopsis mutant that is oversensitive to the effect of nicotinamide on circadian period and identification of the causal mutation in the gene *BIG*. Phenotypic and genotypic analyses of the mutant indicate a wider role for *BIG* in the dynamic adjustment of circadian period. We tested the hypothesis that mutations in this gene that affect the dynamic adjustment of free-running period also affect the entrained phase. We find that this dynamic adjustment of circadian period is associated with establishing the correct phase relationship with the environment. Therefore, our data identify a genetic component required for the correct regulation of circadian period and suggest that circadian period is not fixed at 24 h, thus permitting entrainment to different photoperiods. Our screen has provided important insight into how circadian clocks entrain to environmental cycles and, therefore, how plants tell the time.

RESULTS

A Forward Genetic Screen Identifies Mutants That Are Compromised in Their Ability to Adjust Circadian Period in Response to Nicotinamide

To identify mutants with an altered response of circadian period to nicotinamide, we mutated a Wassilewskija-2 (Ws-2) dual reporter line with ethyl methanesulfonate (EMS), which generates A-G and C-T transitions in base sequence. This line carries both the *CHLOROPHYLL A/B BINDING PROTEIN2 promoter*:*LUCIFERASE*$^+$ (*CAB2*:*LUC*$^+$; Hall et al., 2003) and the *CAULIFLOWER MOSAIC VIRUS 35S promoter*:*APOAEQUORIN* (*35S*:*AEQ*; Xu et al., 2007) reporters. The EMS population was initially screened in the M2 generation for period and amplitude of *CAB2*:*LUC*$^+$ in the presence of 10 mM nicotinamide. We used the *CAB2*:*LUC*$^+$ reporter because this had been used previously to study the effect of nicotinamide on the Arabidopsis circadian clock (Dodd et al., 2007). By measuring the behavior of circadian clock output in *CAB2*, we could examine the consequence of the entire oscillator dynamics, which is not possible when measuring the behavior of a single oscillator component. This screen of 16,000 M2 plants identified 372 putative mutants. These mutants were categorized as follows: *is period insensitive to nicotinamide* (*sin*), *is period oversensitive to nicotinamide* (*son*), or *is amplitude insensitive to nicotinamide* (*san*), based upon a circadian period that was outside of 2 SD of the Ws-2 circadian period (*sin* < 24 h, *son* > 26.1 h) or amplitude (*san* > 0.4 or < 0.18) of *CAB2*:*LUC*$^+$ in the presence of 10 mM nicotinamide. The nature of the M2 screen meant that, in addition to nicotinamide response mutants, it was possible that mutations affecting free-running period also could have been selected.

We performed a rescreen of the M3 generation to confirm initial mutants and exclude those that were just free-running circadian period mutants. In the M3 screen, wild-type Ws-2 plants responded to 20 mM nicotinamide with an increase in circadian period of *CAB2*:*LUC*$^+$ from 23.9 ± 0.2 to 26.2 ± 0.3 h and amplitude reduced from 1.1 ± 0.04 to 0.6 ± 0.03 normalized luminescence counts (n.c.; Fig. 1A). Sixty-three mutants were confirmed by the rescreening of the M3 generation, which also allowed the exclusion of false positives from the M2 screen (Fig. 1B; Supplemental Table S1).

Twenty-five mutants were confirmed for the *sin* phenotype with either no significant period increase in the presence of 20 mM nicotinamide or with a reproducibly smaller increase in period than Ws-2 (Supplemental Table S1). Sixteen mutants were confirmed for the *son* phenotype, with significantly greater period in the presence of 20 mM nicotinamide compared with Ws-2 (Supplemental Table S1). Similarly, 25 *san* mutants were confirmed to have either no significant decrease in amplitude in response to nicotinamide or

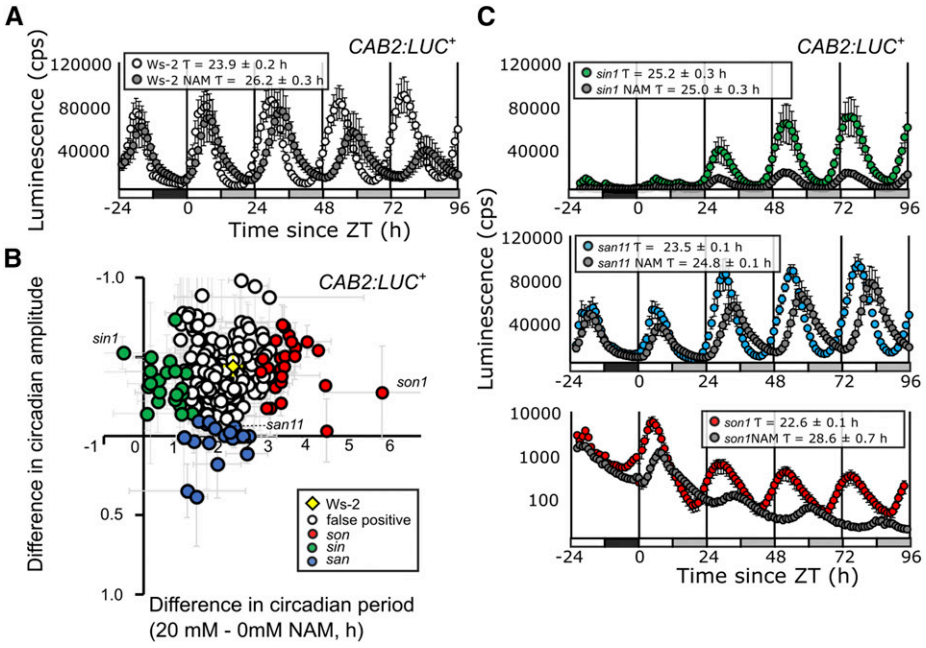

Figure 1. A forward genetic screen separates period and amplitude effects of nicotinamide. A, *CAB2*:*LUC*+ rhythms in wild-type Ws-2 in the presence or absence of 20 mM nicotinamide (NAM) in one entraining 12:12 light/dark cycle (black and white bars) and transferred into 4 d in constant light (white and gray bars) at dawn (Zeitgeber time [ZT] 0). Mean fast Fourier transform-nonlinear least squares (FFT-NLLS) period estimates are shown ± SE (n = 8). B, Free-running circadian period and amplitude difference of M3 plants in a forward genetic screen for the effect of 20 mM nicotinamide on circadian oscillations of *CAB2*:*LUC*+. Period-insensitive mutants (*sin*) are indicated in green, period-oversensitive mutants (*son*) in red, and amplitude-sensitive mutants (*san*) in blue. Plants with no detectable nicotinamide-response phenotype in the screen of the M3 population are shown in white, and the mean wild-type Ws-2 ± SE from all experiments (n = 64) is shown overlaid in yellow. Data are pooled from eight separate experiments. C, *CAB2*:*LUC*+ rhythms in *sin1*, *son1*, and *san11* mutants (labeled in B) in the presence or absence of 20 mM nicotinamide in one entraining 12:12 light/dark cycle and 4 d in 70 µmol m^{-2} s^{-1} constant light (n = 8). Data are representative of two independent experiments in the M3 generation.

significantly smaller amplitude than Ws-2 (Supplemental Table S1).

The strongest phenotypes (Fig. 1C) were seen in *son1*, with a nicotinamide-induced circadian period increase of 6.02 ± 0.75 h (*son1* water, 22.6 ± 0.1 h; 20 mM nicotinamide, 28.6 ± 0.7 h; $P < 0.01$, T = 8.05), *sin1* with no period increase (*sin1* water, 25.2 ± 0.3 h; 20 mM nicotinamide, 25.0 ± 0.3 h; $P = 0.19$, T = 0.92), and *san11*, which had a circadian period increase of 1.3 h but with a rising amplitude of *CAB2*:*LUC*+ compared with damping amplitude in the wild type (*san11* water, 1.08 ± 0.03 n.c.; 20 mM nicotinamide, 1.05 ± 0.0 n.c.; T = 0.83, $P = 0.21$). The *san* lines all had very low amplitude compared with Ws-2 in the absence of nicotinamide, making the phenotypes difficult to measure robustly and map in segregating populations. Therefore, we focused our attention on the *sin* and *son* period mutant classes.

Dose-response curves demonstrated that *son1* was hypersensitive to nicotinamide, with significant increases in circadian period with the addition of 1 mM nicotinamide (Supplemental Fig. S1A; ANOVA: F statistic = 6.87, degrees of freedom [df] = 15, $P = 0.02$), while the Ws-2 circadian period of *CAB2*:*LUC*+ did not vary significantly until the addition of 10 mM nicotinamide (ANOVA: F = 7.85, df = 19, $P < 0.01$). *sin1* was hyposensitive to nicotinamide, as there was no variation in the circadian period of *CAB2*:*LUC*+ between 0.1 mM and 20 mM nicotinamide (Supplemental Fig. S1B; ANOVA: F = 2.15, df = 18, $P = 0.11$). The mutants were backcrossed twice to the parental Ws-2 line carrying *35S*:*AEQ* and *CAB2*:*LUC*+ for mapping. Here, we describe our findings for *son1*, the first mutant that we mapped from the population, which has the strongest phenotype of all those identified.

son1 Maps to a Mutation in a Splice Acceptor in *BIG*

We mapped the causal mutation for *son1* using a mapping population of 25 BC_1F_2 plants clearly displaying the mutant phenotype and sequenced pooled DNA to 50-fold coverage. SHOREmap analysis (Schneeberger et al., 2009) using a sliding window of allele frequency identified a region on the long arm of chromosome 3 where no recombination had occurred (Fig. 2A). Underlying this region was a 750-kb interval containing eight

single-nucleotide polymorphisms (SNPs), with three mutations at positions 433,767, 474,568, and 697,938 predicted to cause functional changes to gene products (Fig. 2B). We confirmed the existence of these SNPs using derived cleaved amplified polymorphic sequence (dCAPS) analysis and Sanger sequencing and fine-mapped the mutation by analyzing the segregation pattern in the BC_2F_3 plants using the M3 screening conditions (Fig 2C; Supplemental Fig. S2). When the segregation pattern of the SNPs was compared with the segregation of the *son1* phenotype, the SNP on chromosome 3 at position 433,767 was the only SNP that segregated with the *son1* phenotype in the BC_2F_3 plants (Fig. 2C; Supplemental Fig. S2, E and F). The wild-type and heterozygous 3:433,767 populations were not distinct from one another, with wild-type period difference (plus and minus nicotinamide) of 1.9 ± 0.5 h and heterozygous period difference of 2.5 ± 0.4 h compared with the homozygous 3:433,767 period difference of 4.3 ± 0.3 h.

This SNP resulted in a G-A transition causing a mutation in the 3′ splice acceptor site of exon 12 of *At3G02260* (Fig. 2D). *At3G02260* encodes BIG, a callosin-like protein of 5,098 amino acids and unknown molecular function (Gil et al., 2001). The M3 line carrying *son1* is slightly short period (Fig. 1). This short-period phenotype in the M3 generation was reproducible but not significant (period difference = 0.53, $P > 0.05$; Supplemental Fig. S3). However, the short-period phenotype was not present in the M4 generation or in the BC_1F_3 (Supplemental Fig. S3) or BC_2F_3 (Supplemental Fig. S2) plants, indicating that the phenotype was not linked to the *son1* phenotype after backcrossing to Ws-2 and that the *son1* mutation does not cause a classical circadian period phenotype

To test the effect of the 3:433,767 mutation on transcript splicing in the *son1* mutant, PCR products were amplified from cDNA using primers spanning exon 11-12 of *BIG* in three independent BC_2F_3 pedigrees. In addition to the 316-bp product amplified from wild-type cDNA (Fig. 2D, lanes 6–8), an additional product was amplified from *son1* mutants (Fig. 2D, lanes 3–5) that was of equivalent size to the 458-bp PCR product amplified from wild-type genomic DNA (Fig. 2D, lane 2), indicating that it represented an unspliced transcript. Sequencing of both *At3G02260* splice variants in *son1* demonstrated that there was a G-A transition corresponding to 3:433,737 in both products (Supplemental Fig. S4). The smaller fragment was 2 bp smaller than the Ws-2 product, with a second AG immediately downstream of the first being used as a splice acceptor instead, while the larger 458-bp product contained the full sequence of intron 11-12, suggesting that it is retained in *son1* due to inefficient splicing. Thus, the G-A 3:433,767 causes both the production of an unspliced transcript and the use of a cryptic splice site in *son1*, both of which result in frame shifts and are predicted to cause premature stop codons.

To confirm that the *son1* phenotype was due to the G-A transition in *BIG*, we assessed the response to nicotinamide in mutants in *BIG* identified from previous mutant screens, *dark overexpresser of cab1-1* (*doc1-1*; Li et al., 1994) and *auxin transport inhibitor response3* (*tir3-101*; Ruegger et al., 1997), using delayed chlorophyll fluorescence (Gould et al., 2009). *doc1-1* has an increase in photosynthesis-related gene expression, including *CAB* genes, in etiolated seedlings in the dark (Li et al., 1994; Gil et al., 2001) caused by a G-A transition resulting in a Cys-to-Thr amino acid substitution in the first Cys-rich domain (CRD-1, also known as a UBR box). *tir3-101* is reported to have impaired polar auxin transport, giving rise to a dwarf phenotype (Ruegger et al., 1997; Prusinkiewicz et al., 2009). Both *doc1-1* and *tir3-101* were oversensitive to nicotinamide compared with their respective wild types (Fig. 2F; Supplemental Fig. S5; Columbia-0 [Col-0], 2.9 ± 0.5 h; *doc1-1*, 4.5 ± 0.4 h; *tir3-101*, 4.4 ± 0.9 h). The increased response of circadian period in the three different *son1*, *doc1-1*, and *tir3-101* alleles of *BIG* suggested that the mutations in *BIG* are causal for the nicotinamide-oversensitive phenotype, and none have a circadian period phenotype in constant high light.

As confirmation, we tested whether *son1* is allelic to *doc1-1*. The *doc1-1 son1* F1 plants had significantly greater period increase in the presence of nicotinamide (4.3 ± 0.7 h) than either Ws-2 (1.7 ± 1.2 h; T = 2.22, df = 19, $P < 0.05$) or Col-0 (2.4 ± 0.6 h; T = 2.16, df = 19, $P < 0.05$) and were not statistically different from either *doc1-1* (4.2 ± 0.4 h; T = 0.22, df = 19, $P = 0.42$) or *son1* (4.9 ± 0.4 h; T = 0.81, df = 19, $P = 0.21$) in the presence of 20 mM nicotinamide (Fig. 2, F and G). To control for ecotype or dominance effects, we analyzed delayed fluorescence in the presence and absence of nicotinamide for F1 of crosses between *son1* and Ws-2, *son1* and Col-0, and *doc1* and Ws-2 (Fig. 2H; Supplemental Fig. S6). These crosses all behaved like the wild type and had circadian period increases that corresponded to the heterozygous BC_2F_3 on the segregation analysis (Fig. 2C). This demonstrates that *doc1-1* is allelic to *son1* and that *BIG* regulates the sensitivity of the circadian oscillator to nicotinamide.

Having established that *son1* and *doc1-1* are both nicotinamide oversensitive for circadian period, we tested whether *son1* plants exhibit the *doc1* phenotype of increased photosynthesis-related gene expression in etiolated seedlings in the dark (Li et al., 1994; Gil et al., 2001). *CAB2*:*LUC*$^+$ expression was higher in etiolated seedlings of *son1* than the wild type in constant dark (Supplemental Fig. S7, A–C), indicating that *son1* also had a dark overexpresser of *CAB* phenotype consistent with allelism to *doc1-1*. Similar to *doc1-1*, higher *CAB2* expression in constant dark was not associated with premature deetiolation (Supplemental Fig. S7, D and E).

To test if BIG could be part of the transcriptional feedback loops of the oscillator, we looked at the transcript profile for *BIG* in the publicly available diurnal transcriptomic data sets under long and short days (Supplemental Fig. S8). *BIG* did not oscillate in either long or short photoperiods in two separate 48-h

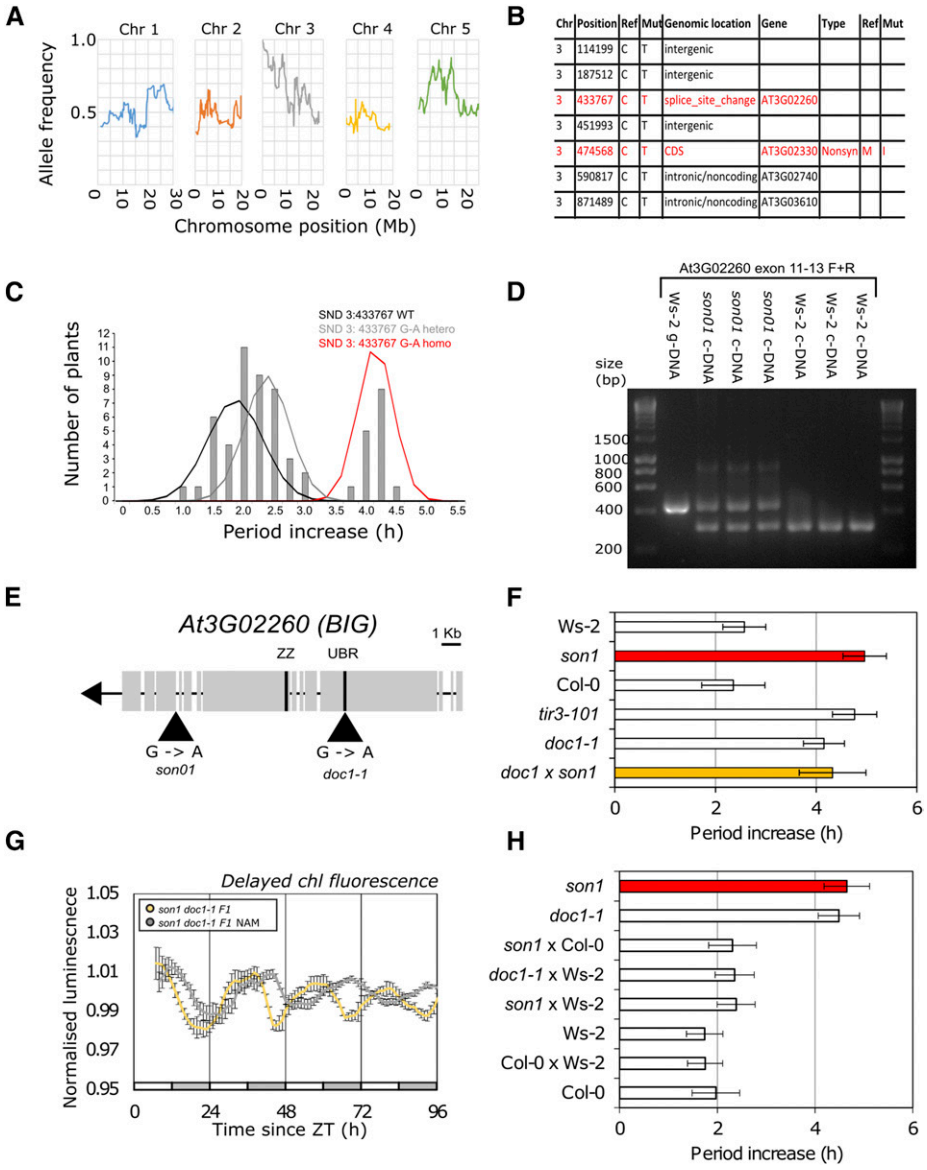

Figure 2. A causal mutation in BIG underlies *son1*. A, SHOREmap backcross mapping by sequencing analysis of *son1* generated from 25-fold coverage Illumina sequence data obtained from 25 BC_1F_2 individual plants with the *son1* phenotype. Individual chromosomes are shown separately with an allele frequency sliding window generated with a moving average of 50 kb. A region with an allele frequency of 1 is found on the long arm of chromosome 3. B, SNPs found on chromosome 3 in *son1* with an allele frequency of 1. Mutations highlighted in red are predicted to cause a functional change in gene product. C, BC_2F_3 segregation of the *son1* phenotype with mutation at 3:433,767. Period difference in the presence of 20 mM nicotinamide was calculated by FFT-NLLS and plotted rounded to the nearest 0.2 h. Each line consisted of eight biological replicates, and 45 lines were genotyped and phenotyped. Mean and SD for each 3:433,767 G-A genotypic subpopulation (wild type [WT], heterozygous, and homozygous) were used to plot normal distributions overlaid onto a period histogram. D, Reverse transcription (RT)-PCR of *BIG* exons 11 to 13 showing the effect of *son1* on *BIG* transcript isoforms. Lane 1 has Ws-2 genomic DNA product of predicted size 458 bp; lanes 2 to 4 have *son1* cDNA products of 314 and 458 bp; lanes 5 to 7 have Ws-2 cDNA product of 316 bp. A 1-kb ladder annotated with fragment sizes is shown. Independently isolated BC_2F_3 pedigrees were used. E, Gene structure of *At3G02260* (*BIG*), the potential UBR- and ZZ-type zinc finger domains, and positions of *son1* and *doc1-1* mutations are labeled. F, Circadian period difference between the presence and absence of 20 mM nicotinamide for delayed chlorophyll fluorescence rhythms in Ws-2, *son1*, Col-0, *doc1-1*, and *son1 doc1-1* F1. Period estimates were calculated using FFT-NLLS analysis (means ± SE; $n = 10$). Data are representative of two independent experiments. G, Delayed chlorophyll fluorescence rhythm for *son1* × *doc1-1* F1 in the presence or absence of 20 mM nicotinamide (NAM) across 4 d in constant light. White and gray bars show subjective day and night. Means ± SE are shown for $n = 10$. Data are representative of two independent crosses. H, Circadian period difference between the presence and absence of 20 mM nicotinamide for delayed chlorophyll fluorescence rhythms of Col-0, Ws-2, Col-0 × Ws-2 F1, *son1*, *doc1*, *son1* × Ws-2 F1, and *doc1* × Ws-2 F1. Period estimates were calculated using FFT-NLLS analysis (means ± SE; $n = 10$).

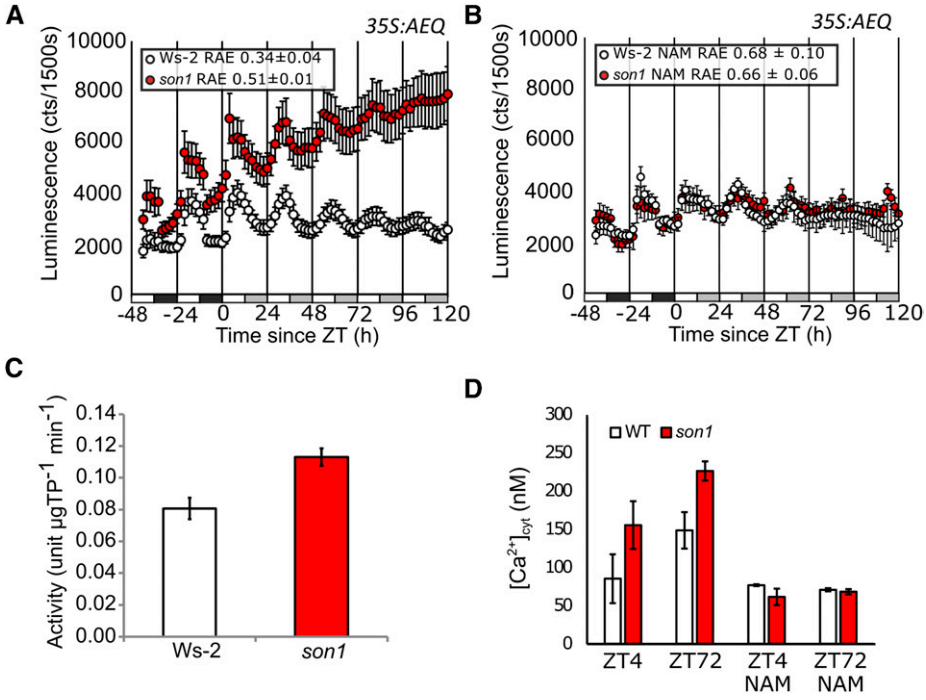

Figure 3. *son1* affects circadian $[Ca^{2+}]_{cyt}$ signals. A and B, Bioluminescence (photon counts per 1,500 s) from *son1* and Ws-2 expressing *35S:AEQUORIN* across two light/dark cycles and 5 d in constant 70 µmol m^{-2} s^{-1} white light grown on 20 mM mannitol (A) or 20 mM nicotinamide (NAM; B). Mean luminescence ± SE is shown; $n = 8$. Data are representative of three independent experiments in the BC_2F_3 generation. C, ADPR cyclase activity measured using nicotinamide guanine dinucleotide assay at ZT4 in 70 µmol m^{-2} s^{-1} white light from 3- to 4-week-old Ws-2 (white) and *son1* (red) seedlings, given as means of three biological replicates shown ± SE. D, $[Ca^{2+}]_{cyt}$ measured at ZT4 and ZT72 in constant 70 µmol m^{-2} s^{-1} white light from 11- and 14-d-old Ws-2 (white) and *son1* (red) seedlings ($n = 12$). Data are representative of three independent experiments in the BC_2F_3 generation. WT, Wild type.

microarray experiments (Mockler et al., 2007; Endo et al., 2014). The abundance of *BIG* transcript also does not appear to be regulated by the circadian oscillator, with no detectable oscillations using JTK_CYCLE ($P > 0.05$) in a circadian transcriptome taken over 48 h in constant conditions (Dalchau et al., 2010). The lack of circadian or diel changes in *BIG* transcript abundance suggests that BIG is not part of the transcriptional feedback loops in the circadian oscillator.

son1 Affects Circadian $[Ca^{2+}]_{cyt}$ Signaling

In addition to increasing circadian period, nicotinamide abolishes the circadian regulation of $[Ca^{2+}]_{cyt}$, potentially through inhibition of the ADPR cyclase activity that generates the Ca^{2+} agonist cADPR (Dodd et al., 2007; Abdul-Awal et al., 2016). We investigated the effect of *son1* on Ca^{2+} signaling using the 35S:AEQ reporter. In Ws-2, there was sinusoidal circadian regulation of $[Ca^{2+}]_{cyt}$, which had an estimated period of 24.2 ± 0.9 h and relative amplitude error (RAE) of 0.3 ± 0 (Fig. 3A). *son1* affected the circadian regulation of $[Ca^{2+}]_{cyt}$, leading to a nonsinusoidal oscillation with an increasing basal level and dampening over time. This resulted in FFT-NLLS analysis estimating the rhythm as only weakly rhythmic, with RAE of 0.5 ± 0.1 (period = 23.1 ± 0.2 h; Fig. 3A). Both *son1* and Ws-2 circadian $[Ca^{2+}]_{cyt}$ signals were inhibited by 20 mM nicotinamide (Fig. 3B; Ws-2, RAE = 0.7 ± 0.1; *son1*, RAE = 0.7 ± 0.1).

Because we have proposed previously that the circadian regulation of $[Ca^{2+}]_{cyt}$ arises from cADPR-mediated Ca^{2+} release, we measured the activity of ADPR cyclase in wild-type and mutant plants. *son1* had significantly higher ADPR cyclase activity compared with Ws-2 ($P = 0.01$) in the middle of the photoperiod representing peak $[Ca^{2+}]_{cyt}$ (Fig. 3C). $[Ca^{2+}]_{cyt}$ also was elevated at the same time point in *son1* compared with Ws-2 (Fig. 3D; $P < 0.05$). This effect was more pronounced after 72 h in constant light, where the 35S:AEQ data previously indicated there to be a much higher basal level of $[Ca^{2+}]_{cyt}$ ($P < 0.05$). $[Ca^{2+}]_{cyt}$ at both time points was reduced by incubation with 20 mM nicotinamide (Fig. 3D). Thus, although nicotinamide reduced $[Ca^{2+}]_{cyt}$ to similar concentrations in the wild type and *son1*, the change in $[Ca^{2+}]_{cyt}$ in *son1* was greater as untreated plants have higher $[Ca^{2+}]_{cyt}$, indicating that the $[Ca^{2+}]_{cyt}$ increase in *son1* might be ADPR cyclase dependent.

son1 Affects Circadian Oscillator Gene Expression

Circadian clocks evolved to provide competitive advantages in light and dark cycles; therefore, to investigate

the role of *BIG* in the daily timing of Arabidopsis, we examined the effect of *son1* on oscillator gene transcript abundance in light and dark cycles and in constant light. As our phenotype was based on the *CAB2* gene, we measured the abundance of *CCA1*, a main circadian regulator of *CAB2*, and also the direct regulators of *CCA1*: *TOC1*, *PRR7*, and *CHE*. *son1* affected circadian oscillator transcript levels in light/dark cycles. The expression of *CCA1* immediately before dawn was higher in *son1* compared with Ws-2 (Fig. 4A; $P < 0.01$), which corresponded to a reduction in *TOC1* expression immediately before dusk (Fig. 4A; $P = 0.01$) and with a significant reduction in *CHE* expression at both dawn and dusk in *son1* (Fig. 4A; $P < 0.01$). We also measured the expression of *CCA1*, *TOC1*, *CHE*, and *PRR7* in constant light across a 48-h time course in *son1* and Ws-2 in the presence and absence of 20 mM nicotinamide and estimated circadian period using JTK_CYCLE (Hughes et al., 2010). We performed this to confirm the *son1* phenotype at the level of gene expression and to identify if there were any changes in gene expression between the mutant and the wild type in the absence of nicotinamide (Fig. 4B). In Ws-2, nicotinamide treatment significantly reduced the peak expression of all the genes in the first cycle ($P < 0.05$). Nicotinamide also significantly reduced peak *CCA1* and *PRR7* transcript levels in *son1*; however, there was no significant change in *TOC1* and *CHE* at any time point. In *son1*, *CCA1* and *PRR7* rhythms had increased circadian period in the presence of nicotinamide compared with Ws-2, with period of 28 h in *son1* ($P < 0.001$) but 24 h in the wild type ($P < 0.001$). *CHE* was not rhythmic with JTK_CYCLE in either Ws-2 ($P = 1$) or *son1* ($P = 0.08$). *TOC1* was rhythmic with JTK_CYCLE in Ws-2, with period of 24 h ($P < 0.05$), but was not rhythmic in *son1* ($P = 0.16$). Thus, the *son1* phenotype can be seen in rhythms of *CCA1* and *PRR7*, but in the presence of nicotinamide, the rhythms of *CHE* and *TOC1* were suppressed, with *TOC1* also being suppressed in *son1* in the absence of nicotinamide.

son1 Affects Dynamic Period Adjustment of the Circadian Oscillator to Regulate the Entrained Phase

As *son1* is compromised in the ability to regulate changes in circadian period in response to nicotinamide, we tested whether it also was affected in its ability to adjust period correctly to other stimuli. Response to light is the most well-characterized dynamic adjustment of the circadian period and is described by Aschoff's rule (Aschoff, 1960). We tested the hypothesis that *son1* might be compromised in the ability to regulate circadian period at different light intensities by performing a fluence response curve (Fig. 5A).

There was no difference between the period length of *CAB2*:*LUC*$^+$ rhythms in Ws-2 and *son1* at 100 µmol m^{-2} s^{-1} light (Ws-2, 23.2 ± 0.1 h; *son1*, 23 ± 0.1 h), which was the intensity of light used for entrainment, indicating again that *son1* is not a circadian period mutant. However, *son1* had a significantly shorter circadian period compared with the wild type under low fluence rates (Fig. 5A; Supplemental Fig. S9): under 5 µmol m^{-2} s^{-1} light, *son1* had a period of 26.6 ± 0.8 h and Ws-2 had a period of 29 ± 0.3 h ($P < 0.01$; Fig. 5B). This indicates that *son1* cannot properly regulate circadian period in response to changes in light intensity. A similar phenotype was detected in *doc1-1*: under 5 µmol m^{-2} s^{-1} light, *doc1-1* had a circadian period of *CAB2*:*LUC*$^+$ of 25.7 ± 0.1 h and Col-0 had a period of 29.2 ± 0.2 h ($P < 0.01$; Supplemental Fig. S9).

Having previously established that *son1* affects the expression of circadian clock genes in a light/dark cycle, we next investigated the effect of *son1* on the entrained phase to investigate the potential roles of *BIG* in the daily timing of Arabidopsis. Wild-type Ws-2 had a typical phase shift of later phase with increasing photoperiod (Fig. 5C, peak at 4.8 ± 0.2 h [8:16], peak at 6.8 ± 0.2 h [12:12], and peak at 8.1 ± 0.2 h [16:8]). By contrast, *son1* was an early phase mutant (Fig. 5, C and D; peak at 3.5 ± 0.2 h [8:16], peak at 5.5 ± 0.2 h [12:12], and peak at 5.7 ± 0.1 h [16:8]). These data demonstrate that *BIG* is required for correct circadian entrainment. Lastly, we measured the effect of nicotinamide on entrained phase under 12:12 (Fig. 5C) and found that it caused a phase delay of *CAB2*:*LUC*$^+$ peak expression of 1 h in Ws-2 and 3 h in *son1* (Ws-2, ZT 7.8 ± 0.2; *son1*, ZT 8.8 ± 0.2), consistent with the effect of nicotinamide on free-running period in both backgrounds.

Finally, having identified that BIG regulates the dynamic adjustment of circadian period and that it is required for correct circadian entrainment, we wanted to investigate whether oscillator period is associated with entrainment and whether the effect of *BIG* on phase could be involved in this regulation. To do this, we studied whether entrainment photoperiod affects free-running period in Ws-2 and *son1* (Fig. 5E). The results showed that there is a relationship between the length of the entrainment photoperiod and the length of the circadian period in Ws-2 (Fig. 5E). However, this relationship was lost in *son1*, whose circadian period was not affected by the duration of the photoperiod during entrainment. As a result of this, *son1* did not have a significantly shorter free-running period of *CAB2*:*LUC*$^+$ compared with Ws-2 when released from entrainment cycles of 8:16 and 12:12 (*son1*, 22.6 ± 0.07 h [8:16] and 22.8 ± 0.14 h [12:12]; Ws-2, 22.7 ± 0.04 h [8:16] and 23.1 ± 0.14 h [12:12]). However, when plants were entrained in 16:8, *son1* had a free-running period of 22.7 ± 0.2 h, 1 h shorter than Ws-2 (23.7 ± 0.06 h; $P < 0.05$; Fig. 5F). This shows that the photoperiod-determined entrained phase of the circadian clock affects the free-running period in constant light, and *son1* does not adjust circadian period correctly in 16:8. We performed the same series of experiments but with circadian free run in constant darkness in the presence of Suc to sustain the oscillation of *CAB2*:*LUC*$^+$ (Dalchau et al., 2011). Similar to the result in constant light, we saw that, in wild-type plants, free-running period length increased with longer entraining photoperiod (Supplemental Fig. S10), and for plants entrained in

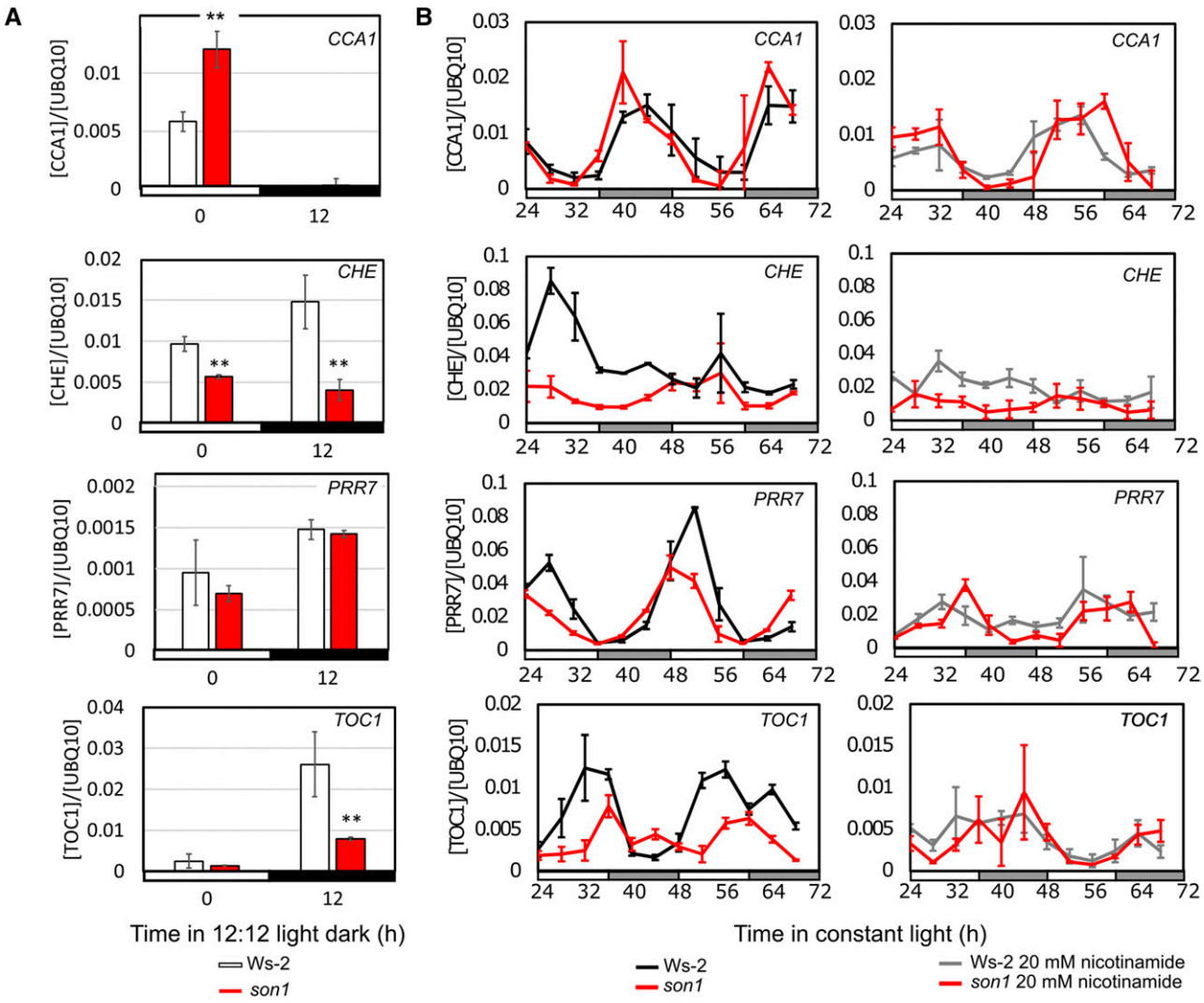

Figure 4. *son1* affects circadian clock gene expression in light/dark cycles and constant light. A, *CCA1*, *PRR7*, *TOC1*, and *CHE* expression from *son1* (red) and Ws-2 (white) samples harvested immediately preceding dawn and dusk. Asterisks represents significance at $P < 0.01$ with Student's *t* test. Relative expression of genes normalized to UBQ10f expression is given ± SD ($n = 3$). B, *CCA1*, *PRR7*, *TOC1*, and *CHE* expression from Ws-2 and *son1* in the absence (left) and presence (right) of 20 mM nicotinamide across 48 h in constant 70 µmol m^{-2} s^{-1} light from ZT24 to ZT72. Relative expression of genes normalized to UBQ10f expression is given ± SD ($n = 3$). Plants were grown as clusters of five plants for 11 d in light/dark cycles prior to the experiment.

16:8, *son1* had a significantly shorter free-running period than the wild type (Ws-2, 27 ± 0.4 h; *son1*, 25.7 ± 0.5 h; $P < 0.05$).

Thus, *son1* cannot correctly adjust period and has impaired phase in response to photoperiod. Collectively, these data demonstrate that nicotinamide targets a pathway involved in establishing the phase relationship between the circadian oscillator and the external environment and that *BIG* contributes to the correct timing of physiology in light/dark cycles, through regulating the pace of the oscillator.

DISCUSSION

Using a forward genetic screen, we found that *BIG* is a regulator of the dynamic adjustment of circadian period and phase. The period of the circadian oscillator is not fixed to 24 h but, instead, is a dynamically plastic phenotype and dependent on environmental conditions. Typically, experimentalists measure circadian period in constant conditions that allow the circadian oscillator to free run. In these constant conditions, the period of the Arabidopsis circadian oscillator decreases with increasing light intensity (Somers et al., 1998b), temperature (Salomé et al., 2010), and Suc (Haydon et al., 2013) and increases with nicotinamide (Dodd et al., 2007). We have identified a nicotinamide-oversensitive phenotype resulting from a mutation in *BIG*. *son1* is allelic to *doc1-1*, a previously characterized mutation in *BIG*, confirming that *BIG* is a regulator of the sensitivity of the circadian oscillator to nicotinamide.

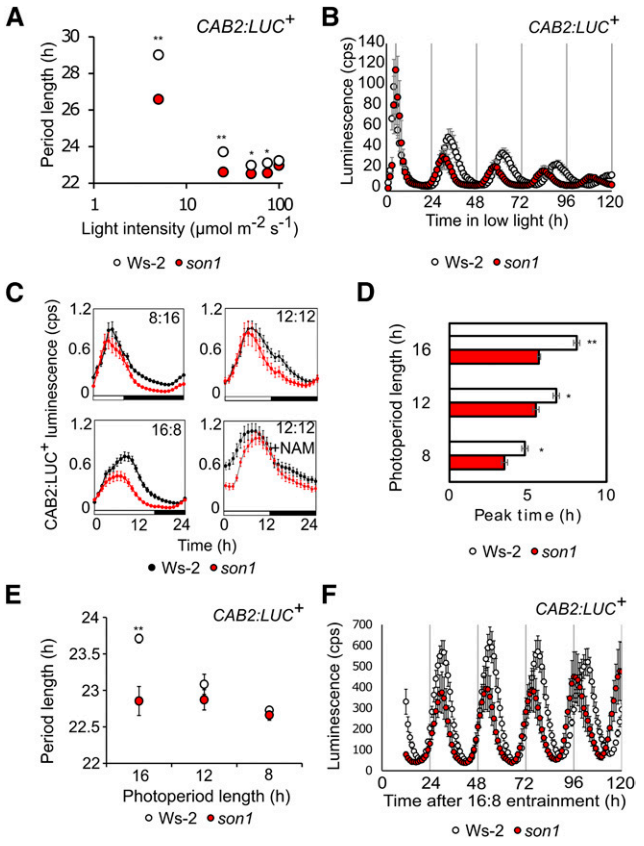

Figure 5. *son1* affects dynamic circadian period adjustment by light and photoperiod. A, Fluence response curve for circadian period of *CAB2*:*LUC*$^+$ in Ws-2 and *son1* estimated in equal mixed red and blue light (means ± SE; n = 8–12). Data are pooled from three independent experiments. B, *CAB2*:*LUC*$^+$ rhythm of *son1* and Ws-2 assayed over 5 d in constant 5 μmol m^{-2} s^{-1} equal mixed red and blue light (means ± SE; n = 8). Data are representative of two independent experiments in the BC_2F_3 generation. In A, the small error bars are obscured by symbols. C, *CAB2*:*LUC*$^+$ luminescence (counts s^{-1}) from *son1* (red) and Ws-2 (black) seedlings grown in 8:16, 12:12, and 16:8 photoperiods. Plants grown in 12:12 were treated with medium supplemented with or without 20 mM nicotinamide (NAM) 2 d prior to entrainment in a camera chamber (means ± SE; n = 8). Plants were grown in entrainment conditions from germination and transferred to the camera chamber 1 d before imaging, maintaining the same entrainment regime. Data are representative of three independent experiments. D, Peak time of *CAB2*:*LUC*$^+$ from the light/dark cycles in C. The mean peak time of CAB2:LUC$^+$ ± SE is plotted (n = 8). E, Photoperiod response curve for the circadian period of *CAB2*:*LUC*$^+$ in Ws-2 and *son1* estimated in equal mixed 80 μmol m^{-2} s^{-1} red and blue light (means ± SE; n = 8). Data are pooled from two independent experiments. Plants were entrained in photoperiods of 16, 12, or 8 h prior to transfer to constant light. F, *CAB2*:*LUC*$^+$ rhythm of *son1* and Ws-2 entrained in a 16:8 light/dark cycle and released into constant light for 5 d (means ± SE; n = 8). Asterisks indicate $P < 0.05$ with Student's t test.

While NAD is an abundant metabolite, we do not suggest that cellular nicotinamide derived from NAD breakdown directly regulates the pace of the circadian oscillator as part of the normal functioning of the plant. Instead, we consider nicotinamide as a probe that can be used to understand the potential mechanisms by which the circadian oscillator dynamically adjusts circadian period. Previously, we proposed that nicotinamide affects circadian period through the inhibition of ADPR cyclase activity and, therefore, the production of cADPR, which is a Ca^{2+} agonist (Dodd et al., 2007; Abdul-Awal et al., 2016). Our demonstration that mutations in *BIG* affecting the sensitivity of the circadian oscillator to nicotinamide also affect the regulation of $[Ca^{2+}]_{cyt}$ are supportive of the hypothesis that nicotinamide regulates circadian period through a Ca^{2+}-sensitive mechanism. *son1* has higher $[Ca^{2+}]_{cyt}$ and ADPR cyclase activity than the wild type, and that increased $[Ca^{2+}]_{cyt}$ is nicotinamide sensitive. This might indicate that the increased effect of nicotinamide on circadian period is related to the altered $[Ca^{2+}]_{cyt}$ in the mutant. However, we do not exclude the possibility of additional Ca^{2+}-insensitive modes of action of nicotinamide on the circadian system (Malapeira et al., 2012).

Animal homologs of BIG, UBR4/p600 in mammals and Calossin/Pushover in *Drosophila melanogaster*, are confirmed calmodulin-binding proteins (Xu et al., 1998; Nakatani et al., 2005; Belzil et al., 2013) and have been proposed to act as part of a Ca^{2+} sensing/signaling mechanism. In mammalian neurons, UBR4, calmodulin, and calmodulin-dependent protein kinase IIα form a complex upon Glu-induced Ca^{2+} entry through NMDA receptors or inositol trisphosphate receptor-mediated Ca^{2+} release from the endoplasmic reticulum (Belzil et al., 2013). Since BIG has a putative calmodulin-binding domain (Yap et al., 2000), it is tempting to speculate that this also could play a role in Ca^{2+} signaling, although the interacting molecular players will be different in plants.

BIG was identified originally as a light signaling regulator (Li et al., 1994) and later was shown to also control multiple hormone signaling pathways (Kanyuka et al., 2003), including auxin transport (Guo and Tan, 2013), and recently was implicated in CO_2-induced stomatal closure (He et al., 2018). The precise biochemical functions of BIG are unknown, but mutations in *Pushover* and knockout or down-regulation of UBR4 also produce pleiotropic phenotypes (Richards et al., 1996; Sekelsky et al., 1999; Yager et al., 2001; Nakatani et al., 2005; Belzil et al., 2014). BIG, UBR4, and Pushover contain a zinc finger-like domain, the UBR box, found in ubiquitin E3 ligases specific to the N-end rule for targeted protein degradation (Gil et al., 2001; Tasaki et al., 2005, 2009). The N-end rule is a conserved pathway in which proteins are targeted for destruction dependent on their N-terminal residue and has diverse roles in different organisms (Bachmair et al., 1986; Gibbs et al., 2014). While UBR4 is required for the degradation of model and physiological N-end rule substrates, it contains no HECT or RING domains and, hence, is considered unlikely to act as an E3 ligase in isolation; rather, it may act as a substrate (N-degron) recognition subunit of a complex (Tasaki et al., 2005, 2009). It is not known whether BIG belongs to an E3 ligase complex or whether it has intrinsic E3 ligase activity. Direct evidence for

the ability of the recombinant UBR box of mammalian UBR4 to bind N-degrons is lacking (Tasaki et al., 2009), but a previous bioinformatics analysis identified a ZZ domain in BIG (Gil et al., 2001). The ZZ domain is structurally and evolutionarily related to the UBR box (Kaur and Subramanian, 2015) and recently was shown to bind N-degrons in the autophagic adaptor protein p62 (Cha-Molstad et al., 2017). There is a precedent for the regulation of circadian period through the control of protein turnover, since a double mutant lacking two ubiquitin-specific proteases, UBP12 and UBP13, exhibits a short-period circadian clock phenotype (Cui et al., 2013). Thus, one potential mode of action of BIG on the circadian oscillator is through a role in protein degradation, but further study will be required to confirm or reject this hypothesis.

The effect of the *son1* mutation on levels of $[Ca^{2+}]_{cyt}$ was greater during the night or subjective night than during the day or subjective day. This is indicative of a time-dependent effect of BIG in the circadian system. Similarly, the *doc1-1* allele of *BIG* specifically affects the expression of *CAB* and other photosynthetic genes at night rather than in the day. These data suggest that *BIG* acts at night in the circadian system. Previous studies have demonstrated that *BIG* plays a role in conveying light information and partially suppresses the phenotype of *phytochromeA* and *phytochromeB* mutations on hypocotyl length (Kanyuka et al., 2003). Thus, *BIG* may be involved in conveying light signaling for circadian entrainment. However, it is likely that *BIG* regulates period or entrainment more widely, due to the effect of *son1* on both nicotinamide period lengthening and photoperiod regulation of period, indicating that *BIG* has a further role outside of light signaling.

Time-dependent effects on the circadian oscillator also are sometimes associated with entrainment, which is the matching of the phase and period of the oscillator with that of the external photoperiod. Synchronization of the circadian oscillator through entrainment ensures that cellular events occur at the right time of day and ensures that the circadian oscillator can track dawn and dusk as they change through the year. This is essential to coordinate whole-organism responses, as circadian period is different between organs (Takahashi et al., 2015) and is age dependent (Kim et al., 2016). We found that *son1* has an early-entrained phase in long-day cycles, suggesting an impact on entrainment. The early phase of *son1* and the reduced ability to dynamically alter circadian period to light and nicotinamide might be related through parametric entrainment. The inability of *son1* to adjust period depending on entrainment photoperiod strongly suggests this. A previous study demonstrated that tissue-specific changes in circadian period are accompanied by corresponding changes in entrained phase (Takahashi et al., 2015). The effect of photoperiod on the entrained phase of the oscillator has been widely reported (Millar and Kay, 1996; Millar et al., 2015; Yeang, 2015). Importantly, Millar et al. (2015) report that the circadian mutant *cca1 lhy* has the same phase under 8:16, 12:12, and 16:8 photoperiods and, thus, is unable to adjust phase to entrainment photoperiod, unlike the wild type, which had a 2.6-h difference. This is similar to the result we find here for *son1*, which has the same phase under 12:12 and 16:8 photoperiods. Unlike *CCA1*, the transcript of *BIG* does not oscillate either in light/dark cycles or in constant light and shows no modulation by photoperiod. This indicates that *BIG* is not part of the transcription-based oscillator loops.

When previously identified Arabidopsis circadian mutants are viewed in the context of phenotypic plasticity to light, they can be assigned to one of four categories (Supplemental Table S2). Mutants can have a constitutive effect on circadian period at all intensities of light; therefore, the mutation has no effect on the dynamic plasticity of the circadian oscillator. Alternatively, mutants might have no plastic response to light, appearing insensitive, with period unchanging at all light intensities. Finally, using the conventions in the literature (Martin-Tryon and Harmer, 2008), we have defined mutations as hyposensitive, with a shallow response curve to light, or hypersensitive, in which the response curve is steep. Ten mutations do not affect dynamic adjustment to either red or blue light, including four mutations that do not affect the response to both wavelengths: the *toc1-1* allele (Somers et al., 1998b), *cry2-1* (Somers et al., 1998a), *fio1-1* (Kim et al., 2008), and *tej* (Panda et al., 2002). There are eight mutations reported to cause insensitivity to either red or blue light, including *prr7-11* to red light (Farré et al., 2005) and *gi-200* (Martin-Tryon et al., 2007) to both red and blue light. Seven mutations cause hypersensitivity to either red or blue light, including *toc1-2* (Martin-Tryon and Harmer, 2008), *lwd1 lwd2* (Wang et al., 2011), and the light-signaling mutants *phyA-201* and *cry1-1* (Somers et al., 1998a). The hypersensitivity in terms of the effect of light on circadian period for *phyA-201* and *cry1-1* is caused by a very steep fluence response curve due to the inability to sense low light intensities. However, only three reported mutations cause hyposensitivity to light. *rve4 rve6 rve8* (Gray et al., 2017) and *phyB-1* (Somers et al., 1998a) confer hyposensitivity to red light, and *prr7-3* confers hyposensitivity to blue light (Farré et al., 2005). The phenotype of *son1* for the white light fluence response curve also is hyposensitive. However, as shown in Supplemental Table S2, *rve4 rve6 rve8* (Gray et al., 2017) and *phyB-1* (Somers et al., 1998a) both have long-period phenotypes in addition to hyposensitivity phenotypes, whereas *son1* has no period phenotype under the light intensity used for the initial entrainment in 12:12 (Fig. 5; Supplemental Fig. S3). Thus, the phenotype of *son1* indicates a function in adjusting period to stimuli, rather than being a core oscillator component, as under normal conditions there is no evidence for it being an oscillator component, since period defects are conditional and the transcript abundance does not oscillate. The short period of *son1* after entrainment only to long days, or through maintenance in

constant low light (Fig. 5) demonstrates that the effect of *son1* is conditional on environmental input, suggesting that BIG is associated with the regulation of the plastic period of the oscillator by environmental signals, rather than acting as a core oscillator component. There is variability in the reported phenotypes of *prr7* mutants, with them being described as long period (Farré et al., 2005) or wild type (Nakamichi et al., 2005; Seki et al., 2017). This and the hyposensitivity to light suggest that *prr7* mutants also might have a defect in plasticity similar to *son1* in terms of responses to light. The mechanisms might be different because PRR7 is an oscillator component, while there is no evidence for BIG being so.

Alterations in circadian period are thought to be required for entrainment, although there is not yet a consensus on how this is achieved. It is envisaged that changes in circadian period are a result of phase adjustment of the oscillator. For example, a phase advance will reduce the period of the cycle in which the advance occurred by an amount equal to the phase advance (Johnson, 1992). Additionally, changes in the velocity of the oscillator can affect period. While changes in period are associated with entrainment, it is not known if this is due to changes in velocity, phase, or both and whether these occur continuously or discontinuously (Daan, 2000). Our discovery of a mutant that is specifically compromised in the ability to dynamically alter circadian period and has altered entrained phase provides a tool with which to study the mechanism of entrainment and the pathways of this essential feature of the circadian oscillator. The study of how the circadian clock establishes a correct phase relationship with the environment is essential to understand the role of the circadian oscillator in the plant, because the timing of events within the diel cycle constitutes the likely evolutionary pressure that resulted in the emergence and optimization of circadian clocks.

MATERIALS AND METHODS

Plant Materials and Growth Conditions

Arabidopsis (*Arabidopsis thaliana*) ecotype Ws-2 carrying *CAB2*:*LUC*$^+$ (Hall et al., 2003) and transformed with *35S*:*AEQ* was described previously (Xu et al., 2007). *doc1-1* (Gil et al., 2001) was obtained from the Nottingham Arabidopsis Seed Stock Centre (Arabidopsis.org). *tir3-101* was a gift from Ottoline Leyser (Sainsbury Laboratory at Cambridge University). Plant growth on agar or soil was as described previously (Xu et al., 2007).

Mutagenesis

Ws-2 seeds homozygous for *CAB2*:*LUC*$^+$ and *35S*:*AEQ* were mutagenized using EMS (Sigma). Seeds were suspended in 150 mM EMS and 0.1% (v/v) KCl for 4 h in an AtmosBag (Sigma). Seeds were washed three times in 100 mM sodium thiosulfate (Fisher) before overnight stratification at 4°C and sowing on soil at a density of 10 seeds per 4 cm^2 of soil. Ten percent of the M1 seedlings had regions of chlorosis, indicative of EMS-induced alterations to the genomic sequence. Seeds were harvested in 10 plant M2 pools. One hundred seeds were screened from 160 pools, with a total of 16,000 M2 seeds screened.

Circadian Phenotyping

Luciferase Imaging

CAB2:LUC$^+$ luminescence was imaged from either clusters of 10 seedlings or individual seedlings (Haydon et al., 2017). Nicotinamide treatment was applied by transferring membranes (1 µm; Sefar) with 7-d-old seedlings to 10 mM nicotinamide-containing medium. Clusters of plants were transferred to nicotinamide-containing plates at 7 d old using a sterile toothpick, lifting plants under the hypocotyls. Treatment with luciferin and imaging with a Nightshade CCD camera and imaging chamber (Berthold) mounted with an 18-mm lens were as described by Haydon et al. (2017). Where the effect of light intensity was investigated, the assay plates were covered with combinations of the following neutral density filters: Lee Technical Filter #211 (Lee Filters) and Roscolux #397, #97, and #98 (Rosco). Light intensity was measured using a Skye Quantum Sensor (Skye Instruments).

Delayed Chlorophyll Fluorescence Imaging

Delayed chlorophyll fluorescence was measured from excised leaves of 28-d-old plants. Leaves were excised at the petiole and transplanted to fresh medium on 25-well plates at dawn. The camera chamber was supplied with constant RB LED light at 70 µmol m^{-2} s^{-1} and was cooled to 20°C. Measurements were automated and data extracted using IndiGO software (Berthold). Delayed chlorophyll fluorescence measurements were taken by acquiring luminescence for 60 s immediately following illumination.

Aequorin Bioluminescence Imaging

Aequorin bioluminescence was imaged from clusters of 15 seedlings as described by Hearn and Webb (2014).

Genetic Mapping

Segregation Analysis

Crosses were made with paternal Ws-2 and maternal mutant. BC_1F_2 seedlings were screened as individual seedlings for circadian period of CAB2:LUC$^+$ on 10 mM nicotinamide. BC_2F_3 seedlings were screened as clusters of seedlings for circadian period of CAB2:LUC$^+$ in the presence or absence of 20 mM nicotinamide.

Mapping by Sequencing

Genomic DNA was extracted from 20-d-old plants using the Qiagen Plant Maxi Kit and quantified using a Nanodrop. Sequencing libraries were prepared using Ilumina Tru-seq. DNA was sequenced by VIB Nucleomics using an Illumina HiSeq 2000. Paired-end reads supplied in fastq format were trimmed using Fast X0.0.13 to remove reads with Q < 20 or read length greater than 35 bp. Adapters were removed using cutadapt 1.2.1. Reads were filtered further to remove those with greater than 90% A content (poly-A reads), all ambiguous reads containing an N in any position, reads with Q < 25, and artifact reads using FastX 0.0.13 and ShortRead 1.20.0. Contaminant reads were removed by discarding reads that aligned to phix_illumina using Bowtie 2.1.0. Sequencing data in fastq format can be obtained from NCBI SRA (ncbi.nlm.nih.gov/sra) under accession SRP119118. Paired-end reads were aligned to the TAIR10 reference genome (Arabidopsis.org) using Bowtie2 version 2.0.2 (Langmead, 2010). SNP calling was performed using SAMtools 0.1.18 mpileup and bcftools (Li, 2011). Vcf files were converted to SHORE format using SHOREmap 2.1 convert. Allele frequency estimation and plots were generated using SHOREmap backcross. The Ws-2 parental strain and Ws-2 1001 Genomes project (http://1001genomes.org/data/MPI/MPIcollab2011/releases/current/strains/Ws-2/) were used for background correction for BC_1F_2 in SHOREmap backcross. SNPs with background frequency less than 16 were discarded. The workflow was automated in a pipeline using bpipe 0.9.8.5. (Supplemental Table S3). Sliding allele frequencies were generated for SNPs based on the R statistic in SHOREmap.

SNP Verification with dCAPS and Sanger Sequencing

Genomic DNA was extracted from 300 µg of plant material using the Plant Mini Kit (Qiagen). DNA was eluted into 150 µL of deionized water (Sigma). dCAPS was used to verify and genotype SNPs in the wild type, BC_1F_2 pools, and BC_2F_3 pedigrees. Primers and restriction enzymes used for dCAPS were as follows, with product sizes once amplicons had been digested given in parentheses: AT3G02260 F, 5′-TTAACATGTAATGTATTCCTCTGCA-3′ and R, 5′-TCCAGTTTCCTCGTTACTGAC-3′, *Hin*dIII 300 bp (276 and 24 bp); AT3G02330 F, 5′-GAGATTTCGTGACCTGGAACG-3′ and R, 5′-GCATCTCTC-GAATAAGCTCTAATG-3′, *Tas*I 300 bp (276 and 24 bp); and AT3G03070 F, 5′-CTAGTCGGCAATCACACCG-3′ and R, 5′-TTTCAGAAATGAACAATTC-CCTGT-3′, *Bsm*I 300 (275 and 25 bp). PCR reagents were purchased as part of the Biotaq Kit (Bioline) or as part of the Phusion Polymerase Kit (New England Biolabs). PCR products were purified using the QIAquick PCR Purification Kit (Qiagen) and quantified using a Nanodrop 2000 (Thermo Scientific). *Hin*dIII (Fisher Scientific), *Tas*I (New England Biolabs), and *Bsm*I (New England Biolabs) reactions were prepared for 100 µg of DNA in their optimal buffers as specified in their instructions. Restriction digestions were run in a Darwin thermocycler for 4 h at 37°C (*Hin*dIII) or 72°C (*Tas*I and *Bsm*I). Restriction enzyme reactions were deactivated by the addition of 4 M Tris, pH 8.4, and purple loading dye (Bioline). Digested and undigested products were run on 2.5% and 4% (w/v) fine molecular biology grade agarose (Bioline) 1× Tris-acetate EDTA buffer for resolution of small fragments. Hyperladder 100 bp (Bioline) was used for size comparison. Gels were imaged using a transilluminator controlled by GeneSnap software with 80-s exposure. Alternatively, purified PCR products were Sanger sequenced using reverse primers as the sequencing primers. Sequencing was performed by Source Bioscience. Sequencing of SNPs was accepted if the chromatograph had a quality score greater than 20.

Isolation of RNA, and Determination of Size and Abundance

RNA Extraction and Reverse Transcription

RNA was extracted using the RNeasy Plant Mini Kit (Qiagen) and the RNase-free DNase set (Qiagen). RNA was double eluted into 30 µL of RNase-free water. cDNA was generated from RNA using the RevertAid First Strand cDNA Synthesis Kit (K1622; Fermentas) using 0.5 µg of RNA in a 10-µL reaction volume.

RT-PCR and RT-Quantitative PCR

Primers were generated using NCBI-primer BLAST as follows: *AT3G02260* F, 5′-GATGGTGAAGCTACTGAGCCT-3′ and R, 5′-CTTCAGCTGGCTC-CATAGCA-3′ (predicted product size for gDNA of 458 bp and for cDNA of 316 bp); UBQ10 F, 5′-GGCCTTGTATAATCCCTGATGAATAAG-3′ and R, 5′-AAAGAGATAACAGGAACGGAAACATAGT; CCA1 F, 5′-GATGATGTT-GAGGCGGATG-3′ and R, 5′-TGGTGTTAACTGAGCTGTGAAG-3′, TOC1 F, 5′-TCTTCGCAGAATCCCTGTGAT-3′ and R, 5′-GCTGCACCTAGCTTCAAG-CA-3′; PRR7 F, 5′-GGAAACTTGGCGGATGAAAA-3′ and R, 5′-CGAGGGC-GTTGTTCTGCT-3′; and CHE F, 5′-TCCACCGGAAATGGTTTTTG-3′ and R, 5′-GGCGGAAGCTTGCTGTTG-3′. RT-PCR was performed using the PCR settings and electrophoresis described above. RT-quantitative PCR was performed as described previously (Haydon et al., 2013).

Cytosol-Free Calcium Measurements

Plants grown on agar plates for 11 d were transferred to cuvettes and dosed with coelenterazine to determine the free Ca^{2+} as described by Martí et al. (2013).

Nicotinamide Guanine Dinucleotide Assay of ADPR Cyclase Activity

ADPR cyclase activity was measured using the nicotinamide guanine dinucleotide assay as described by Abdul-Awal et al. (2016) from 3- to 4-week-old plants grown on agar plates. Rosette tissue (5–10 g) pooled from at least 25 rosettes was harvested as a single biological replicate. Data were collected from three biological replicates.

Estimation of Circadian Parameters

Data were analyzed using the BRASS plug-in for MS Excel (http://www.amillar.org) to carry out FFT-NLLS analysis and manual phase estimation (Plautz et al., 1997). Rhythms were analyzed for at least three cycles in constant light after the first 24 h. FFT-NLLS was performed with period limits between 18 and 35 h at a 95% confidence level. Phase was calculated using the BRASS peak time analysis function. Rhythms in RT-quantitative PCR and microarray time courses were analyzed using JTK_CYCLE (Hughes et al., 2010) with period limits between 20 and 32 h.

Microarray Analysis

Microarray data sets were downloaded from array express (E-GEOD-19271 and E-GEOD-50438) and the DIURNAL long-day and short-day expression sets.

Statistical Tests

Two-sample Student's *t* tests, single-factor ANOVA, and χ^2 statistical tests were performed using MS Excel. The probability of rejecting the null hypothesis (*P*), calculated T, F, or χ^2 statistic, and df are given in the text for each analysis in the form T = *n*, df = *n*, *P* = *n*.

Accession Numbers

Sequence data for the genes used in this study can be found in the Arabidopsis Genome Initiative or GenBank/EMBL databases under the following accession numbers/locus identifiers: BIG (AT3G02260), CAB2 (AT1G29920), CCA1 (AT2G46830), TOC1 (AT5G61380), CHE (AT5G08330), PRR7 (AT5G02810), and ZTL (AT5G57360). Sequencing data in fastq format can be obtained from NCBI SRA (ncbi.nlm.nih.gov/sra) under accession number SRP119118.

Supplemental Data

The following supplemental materials are available.

Supplemental Figure S1. Dose response of circadian period to nicotinamide in Ws-2, *sin1*, and *son1*.

Supplemental Figure S2. *son1* segregates with 3:433,767 in BC_2F_3.

Supplemental Figure S3. *son1* plants do not have a circadian period phenotype in the absence of nicotinamide.

Supplemental Figure S4. Sequencing of cDNA for *son1* fragments.

Supplemental Figure S5. Effects of nicotinamide on delayed chlorophyll fluorescence rhythms in *son1*, *doc1-1*, and *tir3-101*.

Supplemental Figure S6. Allelism of *son1* and *doc1* is not due to ecotype differences.

Supplemental Figure S7. *doc1-1* phenotype in *son1*.

Supplemental Figure S8. *BIG* expression does not oscillate in long- or short-day photoperiods or in constant light.

Supplemental Figure S9. Circadian rhythms of CAB2:LUC^+ in *BIG* mutants under different light intensities.

Supplemental Figure S10. *son1* does not adjust period due to photoperiod entrainment.

Supplemental Table S1. Results of an M3 forward genetic screen for the effect of nicotinamide on the circadian clock.

Supplemental Table S2. Arabidopsis circadian clock genes with circadian and entrainment phenotypes.

Supplemental Table S3. bpipe script for mapping by sequencing.

ACKNOWLEDGMENTS

We thank Ian Henderson for advice on genetic mapping.

Received May 14, 2018; accepted June 28, 2018; published July 11, 2018.

LITERATURE CITED

Abdul-Awal SM, Hotta CT, Davey MP, Dodd AN, Smith AG, Webb AAR (2016) NO-mediated $[Ca2+]_{cyt}$ increases depend on ADP-ribosyl cyclase activity in Arabidopsis. Plant Physiol **171**: 623–631

Aschoff J (1960) Exogenous and endogenous components in circadian rhythms. Cold Spring Harb Symp Quant Biol **25**: 11–28

Ashelford K, Eriksson ME, Allen CM, D'Amore R, Johansson M, Gould P, Kay S, Millar AJ, Hall N, Hall A (2011) Full genome re-sequencing reveals a novel circadian clock mutation in Arabidopsis. Genome Biol **12**: R28

Asher G, Gatfield D, Stratmann M, Reinke H, Dibner C, Kreppel F, Mostoslavsky R, Alt FW, Schibler U (2008) SIRT1 regulates circadian clock gene expression through PER2 deacetylation. Cell **134**: 317–328

Bachmair A, Finley D, Varshavsky A (1986) In vivo half-life of a protein is a function of its amino-terminal residue. Science **234**: 179–186

Belzil C, Neumayer G, Vassilev AP, Yap KL, Konishi H, Rivest S, Sanada K, Ikura M, Nakatani Y, Nguyen MD (2013) A Ca2+-dependent mechanism of neuronal survival mediated by the microtubule-associated protein p600. J Biol Chem **288**: 24452–24464

Belzil C, Asada N, Ishiguro K, Nakaya T, Parsons K, Pendolino V, Neumayer G, Mapelli M, Nakatani Y, Sanada K, (2014) p600 regulates spindle orientation in apical neural progenitors and contributes to neurogenesis in the developing neocortex. Biol Open **3**: 475–485

Cha-Molstad H, Yu JE, Feng Z, Lee SH, Kim JG, Yang P, Han B, Sung KW, Yoo YD, Hwang J, (2017) p62/SQSTM1/Sequestosome-1 is an N-recognin of the N-end rule pathway which modulates autophagosome biogenesis. Nat Commun **8**: 102

Cui X, Lu F, Li Y, Xue Y, Kang Y, Zhang S, Qiu Q, Cui X, Zheng S, Liu B, (2013) Ubiquitin-specific proteases UBP12 and UBP13 act in circadian clock and photoperiodic flowering regulation in Arabidopsis. Plant Physiol **162**: 897–906

Daan S (2000) The Colin S. Pittendrigh Lecture. Colin Pittendrigh, Jürgen Aschoff, and the natural entrainment of circadian systems. J Biol Rhythms **15**: 195–207

Dalchau N, Hubbard KE, Robertson FC, Hotta CT, Briggs HM, Stan GB, Gonçalves JM, Webb AA (2010) Correct biological timing in Arabidopsis requires multiple light-signaling pathways. Proc Natl Acad Sci USA **107**: 13171–13176

Dalchau N, Baek SJ, Briggs HM, Robertson FC, Dodd AN, Gardner MJ, Stancombe MA, Haydon MJ, Stan GB, Gonçalves JM, (2011) The circadian oscillator gene GIGANTEA mediates a long-term response of the Arabidopsis thaliana circadian clock to sucrose. Proc Natl Acad Sci USA **108**: 5104–5109

Dodd AN, Gardner MJ, Hotta CT, Hubbard KE, Dalchau N, Love J, Assie JM, Robertson FC, Jakobsen MK, Gonçalves J, (2007) The Arabidopsis circadian clock incorporates a cADPR-based feedback loop. Science **318**: 1789–1792

Endo M, Shimizu H, Nohales MA, Araki T, Kay SA (2014) Tissue-specific clocks in Arabidopsis show asymmetric coupling. Nature **515**: 419–422

Farré EM, Harmer SL, Harmon FG, Yanovsky MJ, Kay SA (2005) Overlapping and distinct roles of PRR7 and PRR9 in the Arabidopsis circadian clock. Curr Biol **15**: 47–54

Gibbs DJ, Bacardit J, Bachmair A, Holdsworth MJ (2014) The eukaryotic N-end rule pathway: conserved mechanisms and diverse functions. Trends Cell Biol **24**: 603–611

Gil P, Dewey E, Friml J, Zhao Y, Snowden KC, Putterill J, Palme K, Estelle M, Chory J (2001) BIG: a calossin-like protein required for polar auxin transport in Arabidopsis. Genes Dev **15**: 1985–1997

Gould PD, Diaz P, Hogben C, Kusakina J, Salem R, Hartwell J, Hall A (2009) Delayed fluorescence as a universal tool for the measurement of circadian rhythms in higher plants. Plant J **58**: 893–901

Gray JA, Shalit-Kaneh A, Chu DN, Hsu PY, Harmer SL (2017) The REVEILLE clock genes inhibit growth of juvenile and adult plants by control of cell size. Plant Physiol **173**: 2308–2322

Guo Y, Tan J (2013) Applications of delayed fluorescence from photosystem II. Sensors (Basel) **13**: 17332–17345

Hall A, Bastow RM, Davis SJ, Hanano S, McWatters HG, Hibberd V, Doyle MR, Sung S, Halliday KJ, Amasino RM, (2003) The TIME FOR COFFEE gene maintains the amplitude and timing of *Arabidopsis* circadian clocks. Plant Cell **15**: 2719–2729

Haydon MJ, Mielczarek O, Robertson FC, Hubbard KE, Webb AAR (2013) Photosynthetic entrainment of the Arabidopsis thaliana circadian clock. Nature **502**: 689–692

Haydon MJ, Mielczarek O, Frank A, Román Á, Webb AAR (2017) Sucrose and ethylene signaling interact to modulate the circadian clock. Plant Physiol **175**: 947–958

Hazen SP, Schultz TF, Pruneda-Paz JL, Borevitz JO, Ecker JR, Kay SA (2005) LUX ARRHYTHMO encodes a Myb domain protein essential for circadian rhythms. Proc Natl Acad Sci USA **102**: 10387–10392

He J, Zhang RX, Peng K, Tagliavia C, Li S, Xue S, Liu A, Hu H, Zhang J, Hubbard KE, (2018) The BIG protein distinguishes the process of CO_2-induced stomatal closure from the inhibition of stomatal opening by CO_2. New Phytol **218**: 232–241

Hearn TJ, Webb AA (2014) Measuring circadian oscillations of cytosolic-free calcium in Arabidopsis thaliana. Methods Mol Biol **1158**: 215–226

Hong S, Song HR, Lutz K, Kerstetter RA, Michael TP, McClung CR (2010) Type II protein arginine methyltransferase 5 (PRMT5) is required for circadian period determination in Arabidopsis thaliana. Proc Natl Acad Sci USA **107**: 21211–21216

Hughes ME, Hogenesch JB, Kornacker K (2010) JTK_CYCLE: an efficient nonparametric algorithm for detecting rhythmic components in genome-scale data sets. J Biol Rhythms **25**: 372–380

Hunt L, Holdsworth MJ, Gray JE (2007) Nicotinamidase activity is important for germination. Plant J **51**: 341–351

Johnson CH (1992) Phase response curves: what can they tell us about circadian clocks? *In* **T Hiroshige, K Honma**, eds, Circadian Clocks from Cell to Human. Hokkaido University Press, Sapporo, Japan, pp 209–249

Kanyuka K, Praekelt U, Franklin KA, Billingham OE, Hooley R, Whitelam GC, Halliday KJ (2003) Mutations in the huge Arabidopsis gene *BIG* affect a range of hormone and light responses. Plant J **35**: 57–70

Kaur G, Subramanian S (2015) The UBR-box and its relationship to binuclear RING-like treble clef zinc fingers. Biol Direct **10**: 36

Kevei E, Gyula P, Fehér B, Tóth R, Viczián A, Kircher S, Rea D, Dorjgotov D, Schäfer E, Millar AJ, (2007) Arabidopsis thaliana circadian clock is regulated by the small GTPase LIP1. Curr Biol **17**: 1456–1464

Kim H, Kim Y, Yeom M, Lim J, Nam HG (2016) Age-associated circadian period changes in Arabidopsis leaves. J Exp Bot **67**: 2665–2673

Kim J, Kim Y, Yeom M, Kim JH, Nam HG (2008) FIONA1 is essential for regulating period length in the *Arabidopsis* circadian clock. Plant Cell **20**: 307–319

Langmead B (2010) Aligning short sequencing reads with Bowtie. Curr Protoc Bioinformatics **11**: 11.7

Li H (2011) A statistical framework for SNP calling, mutation discovery, association mapping and population genetical parameter estimation from sequencing data. Bioinformatics **27**: 2987–2993

Li HM, Altschmied L, Chory J (1994) Arabidopsis mutants define downstream branches in the phototransduction pathway. Genes Dev **8**: 339–349

Love J, Dodd AN, Webb AAR (2004) Circadian and diurnal calcium oscillations encode photoperiodic information in *Arabidopsis*. Plant Cell **16**: 956–966

Malapeira J, Khaitova LC, Mas P (2012) Ordered changes in histone modifications at the core of the Arabidopsis circadian clock. Proc Natl Acad Sci USA **109**: 21540–21545

Martí MC, Stancombe MA, Webb AAR (2013) Cell- and stimulus type-specific intracellular free Ca2+ signals in Arabidopsis. Plant Physiol **163**: 625–634

Martin-Tryon EL, Harmer SL (2008) XAP5 CIRCADIAN TIMEKEEPER coordinates light signals for proper timing of photomorphogenesis and the circadian clock in *Arabidopsis*. Plant Cell **20**: 1244–1259

Martin-Tryon EL, Kreps JA, Harmer SL (2007) GIGANTEA acts in blue light signaling and has biochemically separable roles in circadian clock and flowering time regulation. Plant Physiol **143**: 473–486

Masuda W, Takenaka S, Inageda K, Nishina H, Takahashi K, Katada T, Tsuyama S, Inui H, Miyatake K, Nakano Y (1997) Oscillation of ADP-ribosyl cyclase activity during the cell cycle and function of cyclic ADP-ribose in a unicellular organism, *Euglena gracilis*. FEBS Lett **405**: 104–106

Millar AJ, Kay SA (1996) Integration of circadian and phototransduction pathways in the network controlling CAB gene transcription in Arabidopsis. Proc Natl Acad Sci USA **93**: 15491–15496

Millar AJ, Carré IA, Strayer CA, Chua NH, Kay SA (1995) Circadian clock mutants in Arabidopsis identified by luciferase imaging. Science **267**: 1161–1163

Millar AJ, Carrington JT, Tee WV, Hodge SK (2015) Changing planetary rotation rescues the biological clock mutant lhy cca1 of Arabidopsis thaliana. bioRxiv

Mockler TC, Michael TP, Priest HD, Shen R, Sullivan CM, Givan SA, McEntee C, Kay SA, Chory J (2007) The DIURNAL project: DIURNAL and circadian expression profiling, model-based pattern matching, and promoter analysis. Cold Spring Harb Symp Quant Biol **72**: 353–363

Nakamichi N, Kita M, Ito S, Yamashino T, Mizuno T (2005) PSEUDO-RESPONSE REGULATORS, PRR9, PRR7 and PRR5, together play essential roles close to the circadian clock of Arabidopsis thaliana. Plant Cell Physiol **46**: 686–698

Nakatani Y, Konishi H, Vassilev A, Kurooka H, Ishiguro K, Sawada J, Ikura T, Korsmeyer SJ, Qin J, Herlitz AM (2005) p600, a unique protein required for membrane morphogenesis and cell survival. Proc Natl Acad Sci USA **102**: 15093–15098

O'Neill JS, van Ooijen G, Dixon LE, Troein C, Corellou F, Bouget FY, Reddy AB, Millar AJ (2011) Circadian rhythms persist without transcription in a eukaryote. Nature **469**: 554–558

Panda S, Poirier GG, Kay SA (2002) tej defines a role for poly(ADP-ribosyl) ation in establishing period length of the Arabidopsis circadian oscillator. Dev Cell **3**: 51–61

Plautz JD, Straume M, Stanewsky R, Jamison CF, Brandes C, Dowse HB, Hall JC, Kay SA (1997) Quantitative analysis of Drosophila period gene transcription in living animals. J Biol Rhythms **12**: 204–217

Prusinkiewicz P, Crawford S, Smith RS, Ljung K, Bennett T, Ongaro V, Leyser O (2009) Control of bud activation by an auxin transport switch. Proc Natl Acad Sci USA **106**: 17431–17436

Ramsey KM, Yoshino J, Brace CS, Abrassart D, Kobayashi Y, Marcheva B, Hong HK, Chong JL, Buhr ED, Lee C, (2009) Circadian clock feedback cycle through NAMPT-mediated NAD+ biosynthesis. Science **324**: 651–654

Richards S, Hillman T, Stern M (1996) Mutations in the Drosophila *pushover* gene confer increased neuronal excitability and spontaneous synaptic vesicle fusion. Genetics **142**: 1215–1223

Ruegger M, Dewey E, Hobbie L, Brown D, Bernasconi P, Turner J, Muday G, Estelle M (1997) Reduced naphthylphthalamic acid binding in the *tir3* mutant of *Arabidopsis* is associated with a reduction in polar auxin transport and diverse morphological defects. Plant Cell **9**: 745–757

Sahar S, Nin V, Barbosa MT, Chini EN, Sassone-Corsi P (2011) Altered behavioral and metabolic circadian rhythms in mice with disrupted NAD+ oscillation. Aging (Albany NY) **3**: 794–802

Salomé PA, Weigel D, McClung CR (2010) The role of the *Arabidopsis* morning loop components CCA1, LHY, PRR7, and PRR9 in temperature compensation. Plant Cell **22**: 3650–3661

Schneeberger K, Ossowski S, Lanz C, Juul T, Petersen AH, Nielsen KL, Jørgensen JE, Weigel D, Andersen SU (2009) SHOREmap: simultaneous mapping and mutation identification by deep sequencing. Nat Methods **6**: 550–551

Sekelsky JJ, McKim KS, Messina L, French RL, Hurley WD, Arbel T, Chin GM, Deneen B, Force SJ, Hari KL, (1999) Identification of novel Drosophila meiotic genes recovered in a *P*-element screen. Genetics **152**: 529–542

Seki M, Ohara T, Hearn TJ, Frank A, da Silva VCH, Caldana C, Webb AAR, Satake A (2017) Adjustment of the Arabidopsis circadian oscillator by sugar signalling dictates the regulation of starch metabolism. Sci Rep **7**: 8305

Somers DE, Devlin PF, Kay SA (1998a) Phytochromes and cryptochromes in the entrainment of the Arabidopsis circadian clock. Science **282**: 1488–1490

Somers DE, Webb AA, Pearson M, Kay SA (1998b) The short-period mutant, toc1-1, alters circadian clock regulation of multiple outputs throughout development in Arabidopsis thaliana. Development **125**: 485–494

Somers DE, Schultz TF, Milnamow M, Kay SA (2000) ZEITLUPE encodes a novel clock-associated PAS protein from Arabidopsis. Cell **101**: 319–329

Takahashi N, Hirata Y, Aihara K, Mas P (2015) A hierarchical multi-oscillator network orchestrates the Arabidopsis circadian system. Cell **163**: 148–159

Tasaki T, Mulder LCF, Iwamatsu A, Lee MJ, Davydov IV, Varshavsky A, Muesing M, Kwon YT (2005) A family of mammalian E3 ubiquitin ligases that contain the UBR box motif and recognize N-degrons. Mol Cell Biol **25**: 7120–7136

Tasaki T, Zakrzewska A, Dudgeon DD, Jiang Y, Lazo JS, Kwon YT (2009) The substrate recognition domains of the N-end rule pathway. J Biol Chem **284**: 1884–1895

Wang Y, Wu JF, Nakamichi N, Sakakibara H, Nam HG, Wu SH (2011) LIGHT-REGULATED WD1 and PSEUDO-RESPONSE REGULATOR9 form a positive feedback regulatory loop in the *Arabidopsis* circadian clock. Plant Cell **23**: 486–498

Xu XZ, Wes PD, Chen H, Li HS, Yu M, Morgan S, Liu Y, Montell C (1998) Retinal targets for calmodulin include proteins implicated in synaptic transmission. J Biol Chem **273**: 31297–31307

Xu X, Hotta CT, Dodd AN, Love J, Sharrock R, Lee YW, Xie Q, Johnson CH, Webb AAR (2007) Distinct light and clock modulation of cytosolic free Ca2+ oscillations and rhythmic CHLOROPHYLL A/B BINDING PROTEIN2 promoter activity in *Arabidopsis*. Plant Cell **19**: 3474–3490

Yager J, Richards S, Hekmat-Scafe DS, Hurd DD, Sundaresan V, Caprette DR, Saxton WM, Carlson JR, Stern M (2001) Control of Drosophila perineurial glial growth by interacting neurotransmitter-mediated signaling pathways. Proc Natl Acad Sci USA **98**: 10445–10450

Yap KL, Kim J, Truong K, Sherman M, Yuan T, Ikura M (2000) Calmodulin target database. J Struct Funct Genomics **1**: 8–14

Yeang HY (2015) Cycling of clock genes entrained to the solar rhythm enables plants to tell time: data from Arabidopsis. Ann Bot **116**: 15–22